ELSEVIER

Journal of Alloys and Compounds 320 (2001) 7–12

Journal of ALLOYS AND COMPOUNDS

www.elsevier.com/locate/jallcom

Exchange interactions in R–Co–B (R=Y, Sm and Gd) compounds

Fumio Maruyama*

177-11, Shimadachi, Matsumoto 390-0852, Japan

Received 11 December 2000; accepted 3 January 2001

Abstract

We calculated the molecular field coefficients, n_{RCo} (R=Sm and Gd) and n_{CoCo} (R=Y) for $R_{n+1}Co_{3n+5}B_{2n}$ (n=0, 1, 2, 3), R_2Co_{17} and $R_2Co_{14}B$ using the experimental values of the Curie temperature. The $R_{n+1}Co_{3n+5}B_{2n}$ compounds with n=1 (RCo_4B), n=2 ($R_3Co_{11}B_4$) and n=3 ($R_2Co_7B_3$) are derived from the RCo_5 structure by substituting B for Co at the 2*c* site. We examined the relationships between the values of n_{RCo} and n_{CoCo} and the B, Co and R concentrations, the Co moments and the two types of volume per formula unit RCo_mB_n and R_mCo_nB.

Keywords: Magnetically ordered materials; Magnetic properties; Exchange interactions

1. Introduction

In rare-earth–transition metal (R–M) compounds, three types of exchange interactions occur: M–M, R–M and R–R. In general, in compounds where the transition metal atoms carry a well established magnetic moment, the M–M interaction dominates. It turns out to be strong enough to produce an almost exact parallel alignment of the 3d magnetic moments at low temperatures. This interaction primarily governs the temperature dependence of the 3d moment and the Curie temperature, T_C, of a 3d–4f compound. The R–M interaction essentially determines the magnetic behavior of the rare-earth sublattice. Due to the localized character of the 4f shell, these R–M interactions are indirect, mediated by the 5d, 6s conduction electrons. The 3d–4f interaction produces a dominant contribution to the molecular field experienced by the rare-earth moments. The R–R interaction between the 4f spins is generally the weakest one in the 3d–4f compounds [1,2].

The $R_{n+1}Co_{3n+5}B_{2n}$ compounds, where R is a rare earth or yttrium, crystallize in a hexagonal structure having the *P6/mmm* space group and are known to exhibit a very interesting series of crystal structures with special atomic orderings depending on n [3–5]. The $R_{n+1}Co_{3n+5}B_{2n}$ compounds with n=1 (RCo_4B), n=2 ($R_3Co_{11}B_4$), n=3 ($R_2Co_7B_3$) and n=∞ (RCo_3B_2) are derived from the RCo_5 structure by substituting B for Co at the 2*c* site [6]. Generally, three kinds of Co atoms are assumed for $R_{n+1}Co_{3n+5}B_{2n}$. Co(0), Co(1) and Co(2) have zero, one and two neighboring B-layers, respectively. The RCo_4B compound has Co(0) and Co(1). The $R_3Co_{11}B_4$ and $R_2Co_7B_3$ compounds have Co(0), Co(1) and Co(2). The RCo_3B_2 compound has only Co(2) and the average Co moment of RCo_3B_2 is very small [7].

The $R_2Co_{14}B$ compound crystallizes with a tetragonal structure having the $P4_2/mnm$ space group. The $R_2Fe_{14}B$ compound is most attractive due to the industrial application for permanent magnets. There are four $R_2Co_{14}B$ units (68 atoms) per unit cell. All the R and B atoms, but only four of the 56 Co atoms, reside in the $z = 0$ and 0.5 planes. Between these the other Co atoms form puckered, yet fully connected, hexagonal nets. The tetragonal structure of $R_2Co_{14}B$ is closely related to the RCo_5-type structure [8].

To compare the strength of the exchange interactions between R and Co spins and between Co spins for R–Co–B and related compounds, we calculated the molecular field coefficients, n_{RCo} (R=Sm and Gd) and n_{CoCo} (R=Y) for $R_{n+1}Co_{3n+5}B_{2n}$ (n=0, 1, 2, 3), R_2Co_{17} and $R_2Co_{14}B$ using the experimental values of the Curie temperature. Moreover, we examined the relationships between the values of n_{RCo} and n_{CoCo} and those of the B, Co and R

E-mail address: vfg04652@nifty.ne.jp (F. Maruyama).

0925-8388/01/$ – see front matter
PII: S0925-8388(01)00939-2

concentrations, the Co moment and the two types of volume per formula unit RCo_mB_n and R_mCo_nB.

2. Results and discussion

The exchange interactions can be analyzed by the molecular field model, which is commonly used to describe the variation of the Curie temperature in the R–Fe intermetallic series, under the assumption that the localized 3d-electron model is applicable.

Applying the two-sublattice molecular field model to the paramagnetic state [1], the following expression can be obtained,

$$T_C = [T_{Co} + T_R + \{(T_{Co} - T_R)^2 + 4T_{RCo}^2\}^{1/2}]/2, \quad (1)$$

where

$$T_{Co} = n_{CoCo}C_{Co}, \quad (2)$$

$$T_R = \alpha^2 n_{RR}C_R, \quad (3)$$

and

$$T_{RCo} = |\alpha| n_{RCo}(C_R C_{Co})^{1/2} = \{(T_C - T_{Co})(T_C - T_R)\}^{1/2}. \quad (4)$$

Here n_{ij} represents the molecular field coefficients, $C_R = N_R g^2 J(J+1)\mu_B^2/3k_B$, N_R is the number of rare-earth atoms per unit volume, $C_{Co} = N_{Co}4S(S+1)\mu_B^2/3k_B$, N_{Co} is the number of Co atoms per unit volume and $\alpha = 2(g-1)/g$. Neglecting T_R, T_C is given by

$$T_C = \{T_{Co} + (T_{Co}^2 + 4T_{RCo}^2)^{1/2}\}/2 \quad (5)$$

and, n_{CoCo} and n_{RCo}, can be calculated using

$$n_{CoCo} = T_{Co}/C_{Co} \quad (6)$$

and

$$n_{RCo} = \{T_C(T_C - T_{Co})/C_R C_{Co}\}^{1/2}/|\alpha|, \quad (7)$$

respectively.

Here, we calculated the molecular field coefficients, n_{RCo}, and n_{CoCo}, for $R_{n+1}Co_{3n+5}B_{2n}$ ($n=0$, 1, 2, 3), R_2Co_{17} and $R_2Co_{14}B$ using the experimental values of T_C. The dependence of the Curie temperature, T_C, on the Co concentration for $R_{n+1}Co_{3n+5}B_{2n}$ ($n=0$, 1, 2, 3), R_2Co_{17} and $R_2Co_{14}B$ (R=Y, Sm and Gd) is shown in Fig. 1. The values of T_C for RCo_5, RCo_4B, $R_3Co_{11}B_4$, $R_2Co_7B_3$, R_2Co_{17} and $R_2Co_{14}B$ are from Refs. [9], [7,10], [7,11], [7,12], [9] and [13], respectively. The values of T_C for R=Y are the smallest. The differences of the values of T_C between those of R=Y and those of R=Sm and Gd for $R_{n+1}Co_{3n+5}B_{2n}$ ($n=1$, 2, 3) are larger than those for RCo_5, R_2Co_{17} and $R_2Co_{14}B$. Taking the value of T_C for the Y compounds as T_{Co}, n_{CoCo} can be deduced using Eq. (6). Then n_{RCo} can be obtained by substituting the appropriate T_C data of each rare-earth compound into Eq. (7).

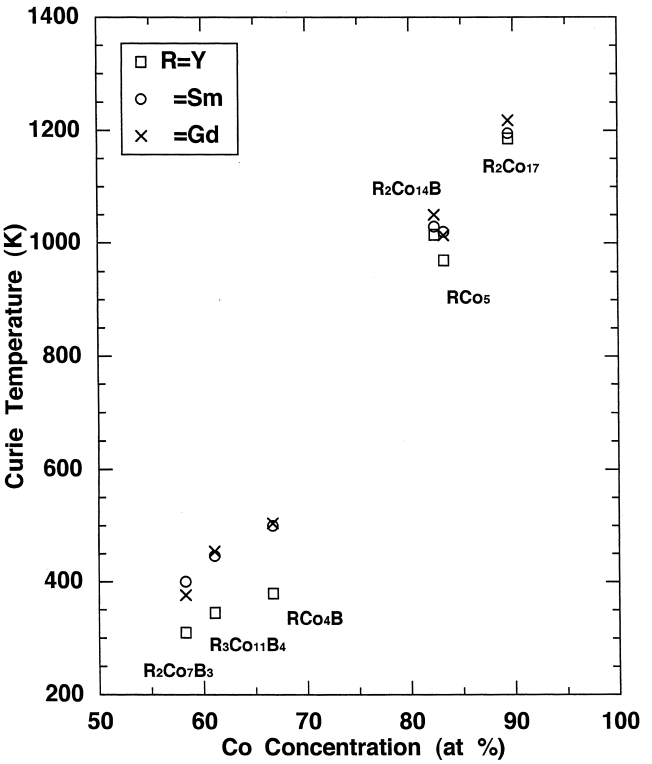

Fig. 1. The dependence of the Curie temperature (T_C) on the Co concentration for $R_{n+1}Co_{3n+5}B_{2n}$ ($n=0$, 1, 2, 3), R_2Co_{17} and $R_2Co_{14}B$ (R=Y, Sm and Gd).

The value of n_{RR} deduced from the ordering temperature for R–Ni compounds is 226 (Oe cm^3/emu) [1]. That is much smaller than the calculated n_{CoCo} and n_{RCo} values for $R_{n+1}Co_{3n+5}B_{2n}$ ($n=0$, 1, 2, 3), R_2Co_{17} and $R_2Co_{14}B$.

The dependence of n_{SmCo}, n_{GdCo}, n_{CoCo} and Co moment, μ_{Co}, on the B concentration for $R_{n+1}Co_{3n+5}B_{2n}$ ($n=0$, 1, 2, 3), R_2Co_{17} and $R_2Co_{14}B$ is shown in Fig. 2. The values of n_{SmCo} and n_{GdCo}, are those of n_{RCo} for R=Sm and Gd, respectively and the values of n_{CoCo} and μ_{Co} are those for R=Y. The values of μ_{Co} for YCo_5, YCo_4B, $Y_3Co_{11}B_4$, $Y_2Co_7B_3$, Y_2Co_{17} and $Y_2Co_{14}B$ are from Refs. [9], [7,10], [7,11], [7,12], [9] and [13], respectively. The value of n_{CoCo} decreases with increasing B content. The values of n_{SmCo} and n_{GdCo} decrease for $R_{n+1}Co_{3n+5}B_{2n}$ ($n=1$, 2, 3) with increasing B content. In rare-earth transition-metal compounds, the exchange coupling of localized 4f and itinerant 3d moments is indirectly promoted via a local 4f–5d interaction combined with an interatomic 5d–3d interaction [14]. The 2p electrons of B lower the density of 3d states at the Fermi level by the 3d–2p hybridization [15] and the values of Co 3d moment decrease, which reduces the effect of 5d–3d hybridization and weakens the 4f–3d exchange interaction, therefore n_{GdCo} decreases. The values of n_{RCo} (R=Sm and Gd) for RCo_5, R_2Co_{17} and $R_2Co_{14}B$ are small in spite of the small B concentration or

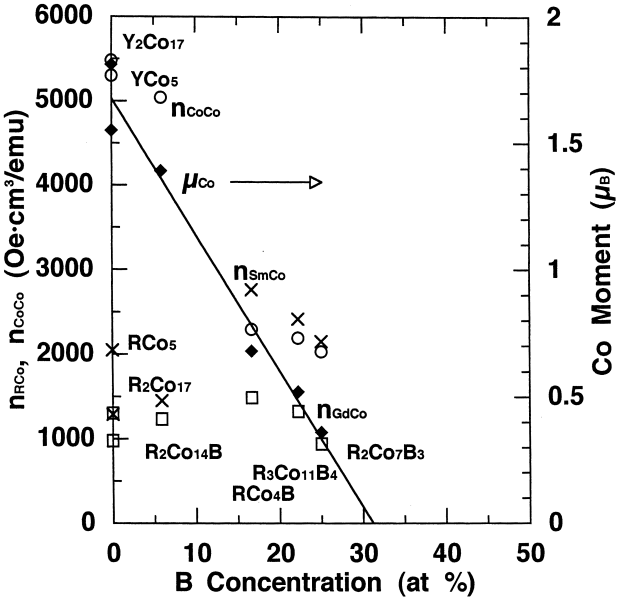

Fig. 2. The dependence of n_{SmCo}, n_{GdCo}, n_{CoCo} and Co moment, μ_{Co}, on the B concentration for $R_{n+1}Co_{3n+5}B_{2n}$ ($n=0$, 1, 2, 3), R_2Co_{17} and $R_2Co_{14}B$.

the absence of B atoms. For those compounds, the Co–Co interaction is strong. The dependence of n_{CoCo} on the B concentration is similar to that of μ_{Co}. The values of n_{CoCo} and μ_{Co} for YCo_5, Y_2Co_{17} and $Y_2Co_{14}B$ are large. The values of n_{CoCo} are approximately proportional to those of T_C.

The dependence of n_{SmCo}, n_{GdCo}, n_{CoCo} and μ_{Co} on the Co concentration for $R_{n+1}Co_{3n+5}B_{2n}$ ($n=0$, 1, 2, 3), R_2Co_{17} and $R_2Co_{14}B$ is shown in Fig. 3. The values of

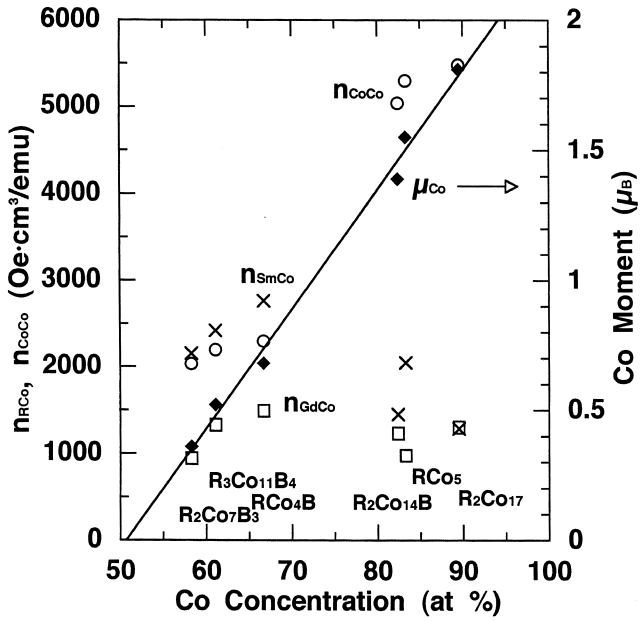

Fig. 3. The dependence of n_{SmCo}, n_{GdCo}, n_{CoCo} and μ_{Co} on the Co concentration for $R_{n+1}Co_{3n+5}B_{2n}$ ($n=0$, 1, 2, 3), R_2Co_{17} and $R_2Co_{14}B$.

μ_{Co} are approximately proportional to those of the Co content. With increasing Co content, the values of n_{SmCo} and n_{GdCo} increase for $R_{n+1}Co_{3n+5}B_{2n}$ ($n=1$, 2, 3) and decrease for RCo_5, R_2Co_{17} and $R_2Co_{14}B$. The value of n_{SmCo} is about two times larger than that of n_{GdCo} except for the values of R_2Co_{17} and $R_2Co_{14}B$. The change in the value of n_{SmCo} is larger than that of n_{GdCo}. With increasing Co content, the values of n_{CoCo}, increase for $Y_{n+1}Co_{3n+5}B_{2n}$ ($n=0$, 1, 2, 3), Y_2Co_{17} and $Y_2Co_{14}B$. The values of n_{CoCo} for $Y_{n+1}Co_{3n+5}B_{2n}$ ($n=1$, 2, 3) are about 2.5 times larger than those for others. For $R_{n+1}Co_{3n+5}B_{2n}$ ($n=1$, 2, 3), the value of n_{SmCo} is larger than that of n_{CoCo}.

The dependence of n_{SmCo}, n_{GdCo} and n_{CoCo} on the R concentration for $R_{n+1}Co_{3n+5}B_{2n}$ ($n=0$, 1, 2, 3), R_2Co_{17} and $R_2Co_{14}B$ is shown in Fig. 4. The values of n_{GdCo} and n_{CoCo} approximately decrease with increasing R content. On the contrary, the value of n_{SmCo} increases with increasing Sm content. In $R_{n+1}Co_{3n+5}B_{2n}$ ($n=0$, 1, 2, 3), for the same R concentration, the values of n_{SmCo} and n_{GdCo} and n_{CoCo} are distributed over a wide range. The value of n_{CoCo} for YCo_5 is much larger considering the Y content. The decrease in the values of n_{CoCo} is larger than that of n_{GdCo}.

A plot of n_{GdCo} versus μ_{Co} for $Gd_{n+1}Co_{3n+5}B_{2n}$ ($n=0$, 1, 2, 3), Gd_2Co_{17} and $Gd_2Co_{14}B$ is shown in Fig. 5. The values of μ_{Co} are obtained by assuming that the Gd moment is 7 μ_B and couples with the Co moment ferrimagnetically. The values of n_{GdCo} are approximately proportional to those of μ_{Co} for $Gd_{n+1}Co_{3n+5}B_{2n}$ ($n=1$, 2, 3) and for $GdCo_5$, Gd_2Co_{17} and $Gd_2Co_{14}B$.

A plot of n_{CoCo} versus μ_{Co} for $Y_{n+1}Co_{3n+5}B_{2n}$ ($n=0$, 1,

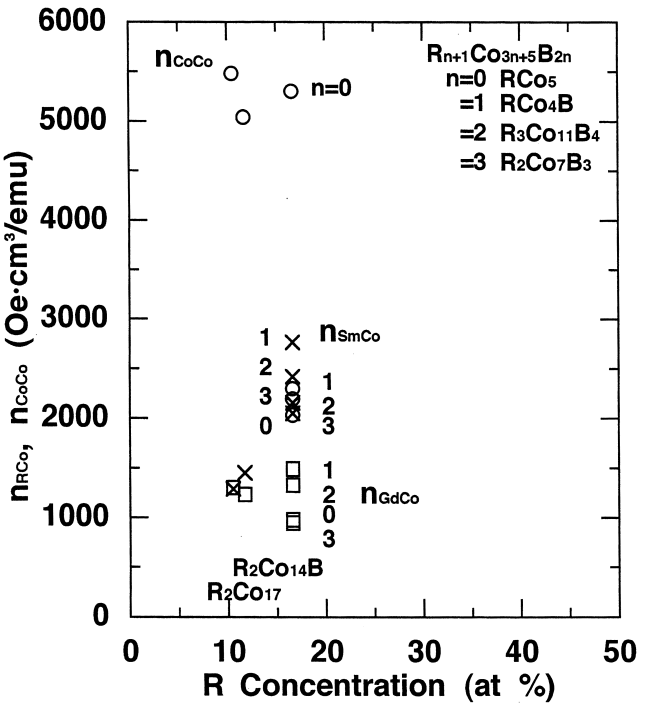

Fig. 4. The dependence of n_{SmCo}, n_{GdCo} and n_{CoCo} on the R concentration for $R_{n+1}Co_{3n+5}B_{2n}$ ($n=0$, 1, 2, 3), R_2Co_{17} and $R_2Co_{14}B$.

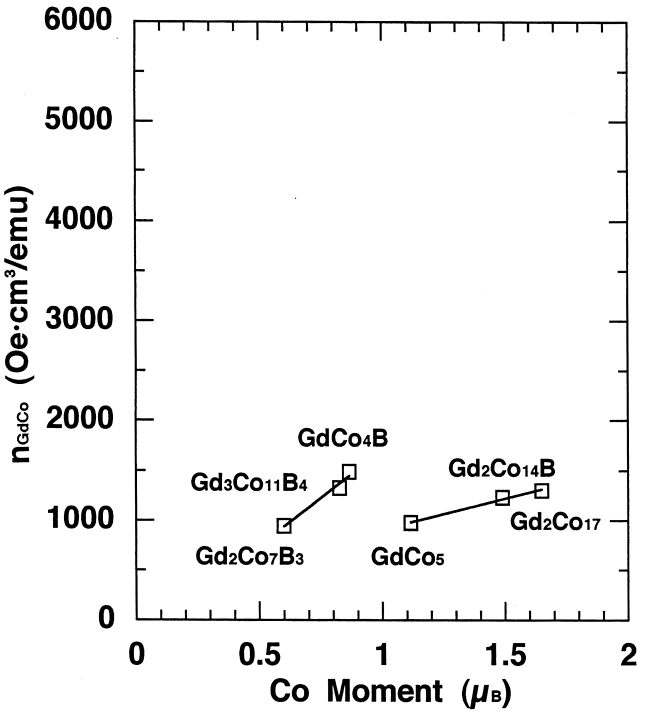

Fig. 5. A plot of n_{GdCo} versus μ_{Co} for $Gd_{n+1}Co_{3n+5}B_{2n}$ ($n=0$, 1, 2, 3), Gd_2Co_{17} and $Gd_2Co_{14}B$.

2, 3), Y_2Co_{17} and $Y_2Co_{14}B$ is shown in Fig. 6. The values of n_{CoCo} increase with increasing μ_{Co}. The values of n_{CoCo} for YCo_5, Y_2Co_{17} and $Y_2Co_{14}B$ are much too large considering the values of μ_{Co}. The value of n_{CoCo} for $Y_2Co_{14}B$ is large in spite of the presence of B atom, because the distance between B and Co is long and therefore the value of μ_{Co} is large (see also Fig. 8).

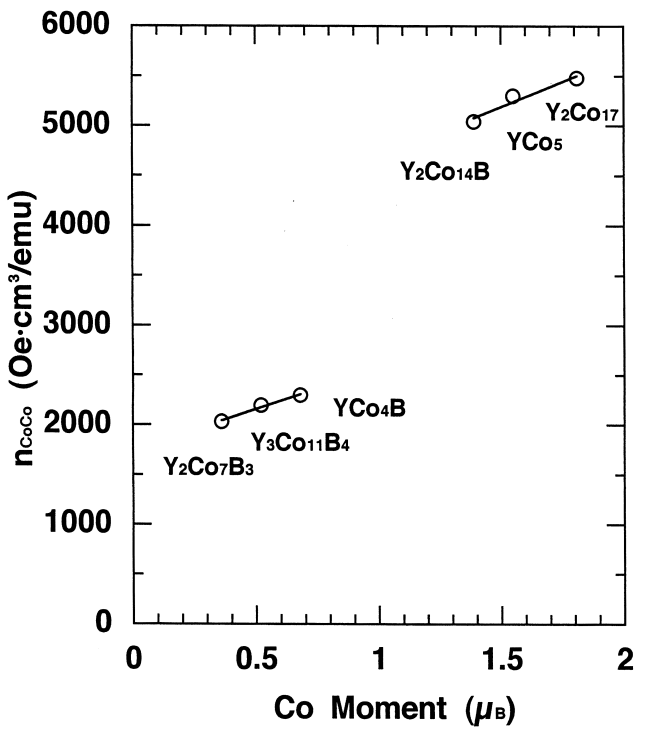

Fig. 6. A plot of n_{CoCo} versus μ_{Co} for $Y_{n+1}Co_{3n+5}B_{2n}$ ($n=0$, 1, 2, 3), Y_2Co_{17} and $Y_2Co_{14}B$.

In view of the different types of unit cells associated with the corresponding crystal structures, we have rewritten the formula composition as RCo_mB_n and used the lattice constants to calculate the volume, V, occupied by one formula unit RCo_mB_n. The values of lattice constants a and c for RCo_5, RCo_4B, $R_3Co_{11}B_4$, $R_2Co_7B_3$, R_2Co_{17} and $R_2Co_{14}B$ are from Refs. [9], [7,10], [7,11], [7,12], [9] and [13], respectively. This V depends on the distance between R and Co. Next, we have rewritten the formula composition as R_mCo_nB and used the lattice constants to calculate the volume, V, occupied by one formula unit R_mCo_nB. This V depends on the distance between Co and B.

The values of n_{SmCo} and n_{GdCo} plotted versus the corresponding reciprocal values of the normalized two types of volume per formula unit RCo_mB_n and R_mCo_nB for $R_{n+1}Co_{3n+5}B_{2n}$ ($n=0$, 1, 2, 3), R_2Co_{17} and $R_2Co_{14}B$ are shown in Fig. 7.

When V is the volume per formula unit RCo_mB_n, the values of n_{GdCo} almost decrease with increasing V^{-1}, but those of n_{SmCo} increase. The change in the values of n_{SmCo} is larger than that of n_{GdCo}. Consequently, with decreasing distances between R and Co, the value of n_{SmCo} increases, which is consistent with the result that the value of n_{SmCo} increases with increasing Sm content as shown in Fig. 4.

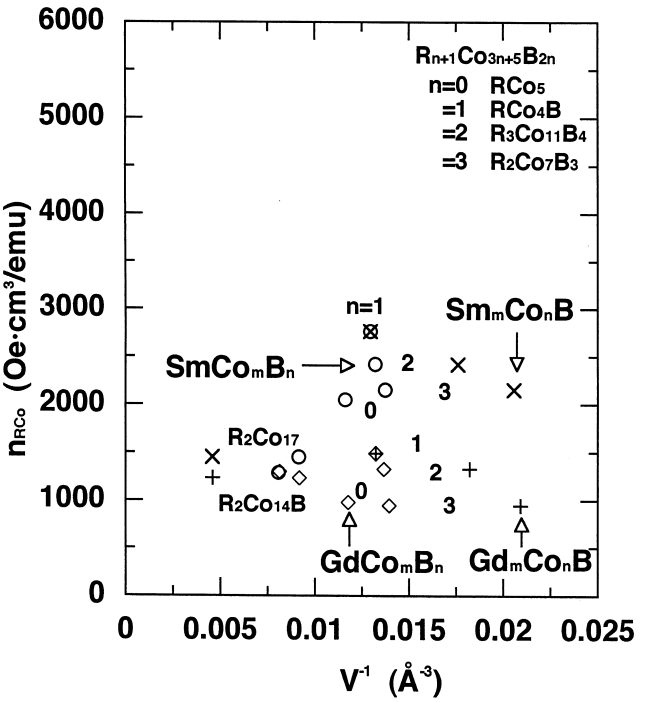

Fig. 7. The values of n_{SmCo} and n_{GdCo} plotted versus the corresponding reciprocal values of the normalized two types of volume per formula unit RCo_mB_n and R_mCo_nB for $R_{n+1}Co_{3n+5}B_{2n}$ ($n=0$, 1, 2, 3), R_2Co_{17} and $R_2Co_{14}B$.

On the contrary, the value of n_{GdCo} decreases. In Ref. [16], the values of n_{ErCo} for $ErCo_3$, Er_2Co_7, $ErCo_4B$, $ErCo_{5.8}$, $Er_2Co_{14}B$, Er_2Co_{17} and $ErCo_{12}B_6$ are roughly proportional to those of V^{-1}. This has been explained in Ref. [16] by assuming that with decreasing V, the 5d–3d hybridization increases and the 4f–3d exchange interaction increases.

When V is the volume per formula unit R_mCo_nB, the values of n_{SmCo} and n_{GdCo} decrease with increasing V^{-1} except for those of $R_2Co_{14}B$. Therefore, with decreasing distances between B and Co, the values of n_{SmCo} and n_{GdCo} decrease for $R_{n+1}Co_{3n+5}B_{2n}$ ($n=1$, 2, 3). When the distance between B and Co becomes small, the 3d–2p hybridization increases and the 3d moment decreases, consequently the 5d–3d hybridization decreases and the 4f–3d exchange interaction weakens. The decrease of the 5d–3d hybridization due to the decreasing 3d moment is larger than the increase of the 5d–3d hybridization due to the decrease of V for R=Gd.

The values of μ_{Co} plotted versus the corresponding normalized cube root of the volume per formula unit YCo_mB_n and per formula unit Y_mCo_nB for $Y_{n+1}Co_{3n+5}B_{2n}$ ($n=0$, 1, 2, 3), Y_2Co_{17} and $Y_2Co_{14}B$ are shown in Fig. 8. In both cases, the values of μ_{Co} are apparently proportional to those of the cube root of V. The decrease of μ_{Co} is particularly large for decreasing values of $V^{1/3}$ in the YCo_mB_n compounds. These results suggest that the values of μ_{Co} are proportional to the distances between Y and Co, and Co and B.

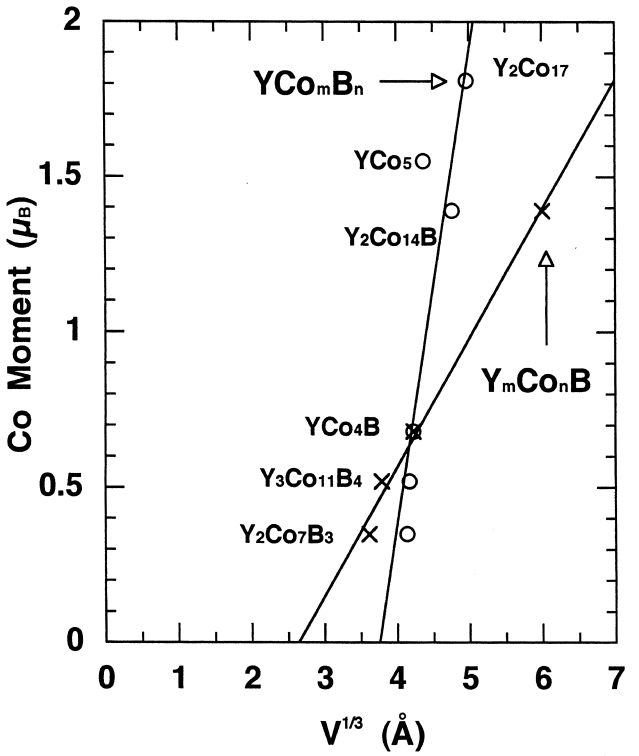

Fig. 8. The values of μ_{Co} plotted versus the corresponding normalized cube root of the volume per formula unit YCo_mB_n and per formula unit Y_mCo_nB for $Y_{n+1}Co_{3n+5}B_{2n}$ ($n=0$, 1, 2, 3), Y_2Co_{17} and $Y_2Co_{14}B$.

The values of n_{CoCo} plotted versus the corresponding reciprocal values of the normalized two types of volume per formula unit YCo_mB_n and per formula unit Y_mCo_nB for $Y_{n+1}Co_{3n+5}B_{2n}$ ($n=0$, 1, 2, 3), Y_2Co_{17} and $Y_2Co_{14}B$ are shown in Fig. 9. In both cases, the values of n_{CoCo} decrease with increasing values of V^{-1}. With increasing distances between Y and Co, and Co and B, the values of μ_{Co} increase (Fig. 8) and also the values of n_{CoCo} increase (Fig. 9). For $Y_2Co_{14}B$ [17], the distances between Co at four sites and B are large, so there are relatively more Co atoms with large moments.

The discussion of the 3d magnetization in rare-earth intermetallics can be performed within the simple concept of magnetic valence Z_m [18]. Within the magnetic valence model, the magnetic moment of an alloy is considered in terms of magnetic moment, M, averaged over all atoms in the alloy. The mean magnetic moment per atom M is expressed as

$$M = Z_m + 2N_{sp}^{\uparrow}. \quad (8)$$

Here Z_m is the magnetic valence; $2N_{sp}^{\uparrow}$ is the number of s and p electrons in the spin-up-state band. The values of $N_{sp}^{\uparrow}$ usually range from 0.3 to 0.45 [18]. Z_m is expressed as

$$Z_m = 2N_d^{\uparrow} - Z. \quad (9)$$

Here $N_d^{\uparrow}$ is the number of electrons in the spin-up band and Z is the chemical valence. To apply the magnetic valence

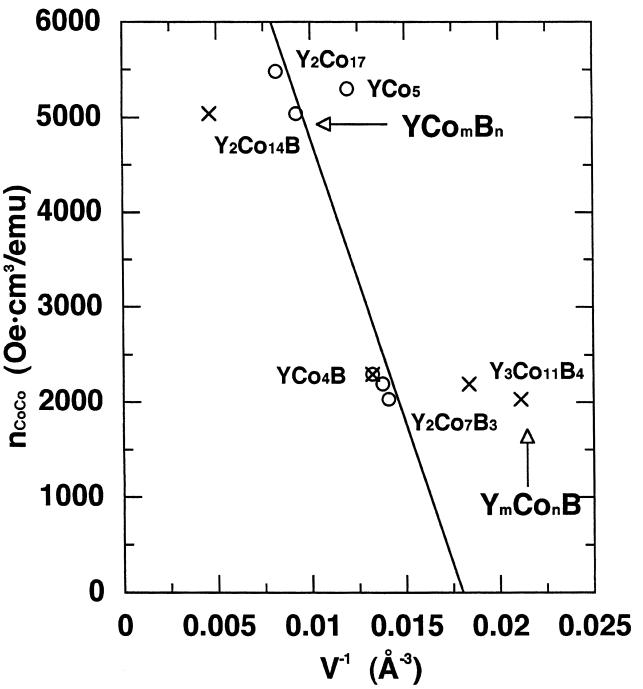

Fig. 9. The values of n_{CoCo} plotted versus the corresponding reciprocal values of the normalized two types of volume per formula unit YCo_mB_n and per formula unit Y_mCo_nB for $Y_{n+1}Co_{3n+5}B_{2n}$ ($n=0$, 1, 2, 3), Y_2Co_{17} and $Y_2Co_{14}B$.

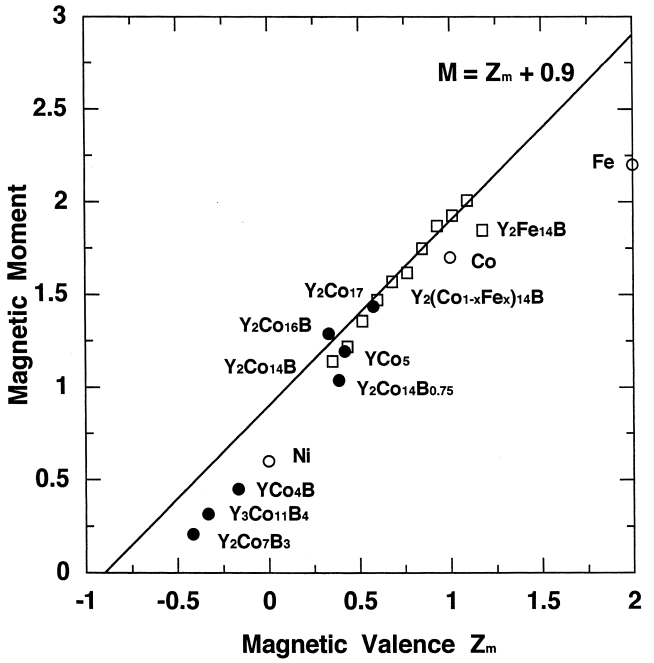

Fig. 10. The experimental magnetic moment as a function of magnetic valence for Y–Co–B, Y–Co, Y–Co–Fe–B, Fe, Co and Ni and the calculated moments with $N_{sp}^{\uparrow} = 0.45$, with strong ferromagnetism, in Eq. (8).

model, the Y–Co–B series can be rewritten as $Y_{y1}Co_{1-y}B_{y2}$ ($y = y1 + y2$). Then Z_m is expressed as

$$Z_m = 2N_d^{\uparrow}(1-y) - Z_{Co}(1-y) - (Z_Y y1 + Z_B y2). \quad (10)$$

Here $N_d^{\uparrow}$ is taken to be the value for a strong ferromagnet (=5). The values of chemical valence are $Z_{Co}=9$, $Z_Y=3$, $Z_B=2$ [18].

The experimental magnetic moment as a function of magnetic valence for Y–Co–B, Y–Co, Y–Co–Fe–B, Fe, Co and Ni and the calculated moments with $N_{sp}^{\uparrow} = 0.45$, with strong ferromagnetism, in Eq. (8) are presented in Fig. 10. The values of the experimental magnetic moment for $Y_2(Co_{1-x}Fe_x)_{14}B$, $Y_2Co_{14}B_{0.75}$ and $Y_2Co_{16}B$ are from Refs. [19,20] and [17], respectively. For $Y_{n+1}Co_{3n+5}B_{2n}$ ($n=1, 2, 3$), the experimental magnetic moment is below the calculated one, which shows that weak ferromagnetism is present. For YCo_5 and Y_2Co_{17}, the experimental magnetic moment is near the calculated one, hence whose compounds show strong ferromagnetism. For $Y_2(Co_{1-x}Fe_x)_{14}B$, a transition from weak to strong ferromagnetism occurs as x increases from 1 to 0.9.

3. Conclusions

We calculated the molecular field coefficients, n_{RCo}, (R=Sm and Gd) and n_{CoCo} (R=Y) for $R_{n+1}Co_{3n+5}B_{2n}$ ($n=0, 1, 2, 3$), R_2Co_{17} and $R_2Co_{14}B$ using the experimental values of the Curie temperature.

With increasing B content, the value of n_{CoCo} decreases. The values of n_{SmCo} and n_{GdCo} decrease for $R_{n+1}Co_{3n+5}B_{2n}$ ($n=1, 2, 3$). With increasing Co content, the values of n_{SmCo} and n_{GdCo} increase for $R_{n+1}Co_{3n+5}B_{2n}$ ($n=1, 2, 3$) and decrease for RCo_5, R_2Co_{17} and $R_2Co_{14}B$ and those of n_{CoCo} increase. With increasing R content, the values of n_{GdCo} and n_{CoCo} approximately decrease, but the value of n_{SmCo} increases.

With decreasing distances between R and Co, the value of n_{SmCo} increases and that of n_{GdCo} decreases. With decreasing distances between B and Co, the values of n_{SmCo} and n_{GdCo} decrease for $R_{n+1}Co_{3n+5}B_{2n}$ ($n=1, 2, 3$).

The values of μ_{Co} are proportional to the distances between Y and Co, and Co and B. With increasing distances, the values of μ_{Co} increase and those of n_{CoCo} increase.

The tendency of the values of n_{RCo} and n_{CoCo} for $R_{n+1}Co_{3n+5}B_{2n}$ ($n=1, 2, 3$) is different from that for RCo_5, R_2Co_{17} and $R_2Co_{14}B$.

References

[1] E. Belorizky, M.A. Fremy, J.P. Gavigan, D. Givord, H.S. Li, J. Appl. Phys. 61 (1987) 3971.
[2] J.J.M. Franse, R.J. Radwanski:, in: K.H.J. Buschow (Ed.), Handbook of Magnetic-Materials, Vol. 7, North-Holland, Amsterdam, 1993, p. 307.
[3] H. Osterreicher, F.T. Parker, M. Misroch, Appl. Phys. 12 (1977) 287.
[4] Y.B. Kuzma, N.S. Bilonizhko, S.I. Mykhalenko, G.F. Stepanova, N.F. Chaban, J. Less-Common Metals 67 (1979) 51.
[5] H.H. Smit, R.C. Thiel, K.H.J. Buschow, J. Phys. F 18 (1988) 295.
[6] Y.B. Kuzma, N.S. Bilonizhko, Soy. Phys. Crystallogr. 18 (1974) 447.
[7] H. Ido, Kotai Butsuri 30 (1995) 875, in Japanese.
[8] D. Givord, H.S. Li, J.M. Moreau, Solid State Commun. 50 (1984) 497.
[9] K.H.J. Buschow, Rep. Prog. Phys. 40 (1977) 1179.
[10] H.S. Li, J.M.D. Coey, in: K.H.J. Buschow (Ed.), Handbook of Magnetic Materials, Vol. 6, North-Holland, Amsterdam, 1991, p. 1.
[11] A. Kowalczyk, J. Magn. Magn. Mater. 136 (1994) 70.
[12] A. Kowalczyk, J. Magn. Magn. Mater. 175 (1997) 279.
[13] K.H.J. Buschow, D.B. de Mooij, S. Sinnema, R.J. Radwanski, J.J.M. Franse, J. Magn. Magn. Mater. 51 (1985) 211.
[14] M.S.S. Brooks, O. Eriksson, B. Johanson, J. Phys. Condens. Matter 1 (1989) 5861.
[15] M. Aoki, H. Yamada, Physica B 177 (1992) 259.
[16] J.P. Liu, F.R. de Boer, P.F. de Chatel, R. Coehoom, K.H.J. Buschow, J. Magn. Magn. Mater. 132 (1994) 159.
[17] F. Maruyama, H. Nagai, Y. Amako, H. Yoshie, K. Adachi, Jpn. J. Appl. Phys. 35 (1996) 6057.
[18] J.P. Gavigan, D. Givord, H.S. Li, J. Voiron, Physica B 149 (1988) 345.
[19] F. Maruyama, H. Nagai, K. Adachi, J. Phys. Soc. Jpn. 62 (1993) 3741.
[20] F. Maruyama, H. Nagai, Y. Amako, H. Yoshie, K. Adachi, Jpn. J. Appl. Phys. 34 (1995) 1542.